Research Article

Zaki Mrzog Alaof, Khalid K. Ali*, Mona S. Mehanna, Abdel-Haleem Abdel-Aty, and Mohamed A. Shaalan

Applications of the Belousov–Zhabotinsky reaction–diffusion system: Analytical and numerical approaches

https://doi.org/10.1515/phys-2025-0129
received August 22, 2024; accepted February 17, 2025

Abstract: The Belousov–Zhabotinsky (BZ) reaction–diffusion system is a well-known model of chemical self-organization that exhibits complex spatiotemporal patterns. The BZ reaction–diffusion system provides a useful tool for studying the behavior of waves in random and complex media. Its applications in this field are wide-ranging and have the potential to contribute to a better understanding of the behavior of waves in natural and engineered systems. In this article, we investigate the BZ system using both analytical and numerical methods. We first apply the Bernoulli sub-ordinary differential equation (ODE) technique to the BZ system to obtain a simplified system of ODEs. Then, we use the exponential cubic B-spline method and the trigonometric cubic B-spline method to solve the simplified system numerically. The results show that both methods are effective in capturing the essential features of the BZ system. We also compare the results obtained using the two numerical methods. Our findings analytically contribute to a better understanding of the BZ system through graphs of the soliton solutions.

Keywords: Belousov–Zhabotinsky reaction–diffusion model, Bernoulli sub-ODE technique, soliton solutions, exponential cubic B-spline method, trigonometric cubic B-spline method

*** Corresponding author: Khalid K. Ali,** Mathematics Department, Faculty of Science, Al-Azhar University, Nasr-City, Cairo, Egypt, e-mail: khalidkaram2012@azhar.edu.eg
Zaki Mrzog Alaof: Department of Mathematics, Applied College at Mahail Aseer, King Khalid University, Abha, Saudia Arabia, e-mail: zaleawfi@kku.edu.sa
Mona S. Mehanna: Faculty of Engineering, MTI University, Cairo, Egypt, e-mail: monamehanna@gmail.com
Abdel-Haleem Abdel-Aty: Department of Physics, College of Sciences, University of Bisha, PO Box 344, Bisha 61922, Saudi Arabia; Physics Department, Faculty of Science, Al-Azhar University, Assiut 71524, Egypt, e-mail: amabdelaty@ub.edu.sa
Mohamed A. Shaalan: Higher Technological Institute, Tenth of Ramadan City, Egypt, e-mail: mohamed.abozaid@hti.edu.eg

1 Introduction

The Belousov–Zhabotinsky (BZ) system was first discovered in the 1950s by Boris Belousov, a Russian chemist, who observed an unusual color change in a mixture of chemicals. Later, Anatol Zhabotinsky expanded on Belousov's work and discovered that the reaction could produce oscillations and other dynamic patterns. The BZ reaction is described by a system for the first time in 1983 [1]. The BZ reaction–diffusion system is a well-known example of a chemical oscillator that exhibits periodic and chaotic behavior. The system involves the oxidation of a reducing agent by a chemical oxidant, with the product of the reaction then oxidizing the original reducing agent in a cyclic process. This process is accompanied by a change in the concentration of one or more species over time. The BZ reaction–diffusion system can also exhibit spatial patterns, which can be modeled using a reaction–diffusion system. In this system, the concentration of the reactants and products is allowed to vary both in time and space and is governed by a set of partial differential equations. The BZ reaction–diffusion system is notable for its ability to produce a wide variety of complex spatiotemporal patterns, including spirals, stripes, and spots. The system has been studied extensively both experimentally and mathematically and has applications in fields such as chemistry, physics, and biology. The BZ reaction illustrates oscillatory behavior in chemical reactions and is a famous example of non-equilibrium thermodynamics. Because of the fluctuating reactant and product concentrations, this reaction, which includes the interaction of bromate ions with organic acids, causes periodic color variations. The BZ reaction has a wide range of physical phenomena, from biological systems to materials science and environmental science, including modeling the electrical impulses that regulate heartbeats, creating self-assembling materials with complex structures and modeling the spread of pollutants in water bodies [2–4]. The study of the BZ reaction–diffusion system has led to important insights into the behavior of complex chemical systems and has inspired the development of new mathematical and computational techniques for studying these systems. The system continues to be an active area of research, with new applications and insights being discovered all the time. The principle idea that the main factor determining the wavefront's speed is how concentrated certain chemical substances, the bromous acid ($HBrO_2$) and the bromide ion (Br^-) given by U and V, respectively. The sequence of simplified reaction

$$A + \mathsf{V} \rightleftharpoons^{k_1} \mathsf{U} + P, \quad \mathsf{U} + \mathsf{V} \rightleftharpoons^{k_2} 2P,$$
$$A + \mathsf{U} \rightleftharpoons^{k_3} 2\mathsf{U}, \quad 2\mathsf{U} \rightleftharpoons^{k_4} P + A,$$

where k_1, k_2, k_3, and k_4 are known rate constants, P is the compound HBrO, and A is the concentration of BrO_3^-. By using lowercase letters for concentrations, applying the Law of Mass Action to this scheme

$$\mathsf{U}_x = k_1 a\mathsf{V} - k_2\mathsf{UV} + k_3 a\mathsf{U} - k_4\mathsf{U}^2 + D\mathsf{U}_{xx},$$
$$\mathsf{V}_t = -k_1 a\mathsf{V} - k_2\mathsf{UV} + D\mathsf{V}_{xx},$$

where D is the diffusion coefficient. A suitable non-dimensional is

$$\theta = \frac{k_4\mathsf{U}}{k_3 a}, \quad v = \frac{k_2\mathsf{V}}{k_3 ar}, \quad x^* = \left(\frac{k_3 a}{D}\right)^{\frac{1}{2}} x$$
$$t^* = k_3 at, \quad L = \frac{k_1 k_4}{k_2 k_3}, \quad M = \frac{k_1}{k_3}, \quad b = \frac{k_2}{k_4},$$

where the parameter r is used to describe the concentration of bromide ions in the BZ reaction and can be experimentally manipulated. We omit the asterisks for simplicity

$$\theta_t = Lrv + \theta(1 - \theta - rv) + \theta_{xx},$$
$$v_t = -Mv - b\theta v + v_{xx},$$

since $L \approx M = O(10^{-4})$, $L \ll 1$, and $M \ll 1$, We simplify the model for the BZ reaction by disregarding these terms. The resulting model is described by a system of equations

$$\theta_t = \theta_{xx} + \theta(1 - \theta - rv),$$
$$v_t = v_{xx} - b\theta v,$$

we search for traveling wavefront solutions in the BZ reaction in which the level of bromide ion is lowered and the wave travels from a zone of high bromous acid concentration to one of low bromous acid concentration. So, we apply appropriate boundary conditions to solve the BZ system

$$\theta(-\infty, t) = 0, \quad v(-\infty, t) = 1, \quad \theta(\infty, t) = 1, \quad v(\infty, t) = 0,$$

where the functions θ and v introduce the bromous acid and bromide ion concentrations, respectively. r and b are positive constants, for more details see [5]. We employ the variable change $\Theta = \theta$ and $\mho = 1 - v$ [6], which results in

$$\Theta_t = \Theta_{xx} + \Theta(1 - r - \Theta + r\mho),$$
$$\mho_t = \mho_{xx} + b\Theta(1 - \mho). \tag{1}$$

The traveling wave solutions are studied under different conditions by various researchers: Murray [7,8], Tyson [9], Ye and Wang [10,11], Li [12], Li and Ye [13], Trofimchuk *et al.* studied the stability and the uniqueness of monotone wave fronts [14]; Basavaraja *et al.* investigated oscillating patterns and bifurcation phase diagrams for the BZ system [15], Manoranjan and Mitchell [16] used the finite-element method to obtain the wave solution; Wang *et al.* [17] presented solutions for four kinds of explicit wavefronts. Quinney presented the soliton solutions using the finite-difference method [18]. The soliton solutions can be investigated by a variety of analytical methods, like the Bernoulli sub-ordinary differential equation (ODE) method [19], Laplace transform method [20], and Hirota bilinear method [21,22]. The authors [23–26] have mentioned several numerical methods, including parametric continuation, shooting, finite difference, and basis spline functions collocation methods. These analytical and numerical methods are commonly used in various fields and can be applied to solve a wide range of problems.

This work is organized into several sections. In Section 2, we present a summary of the analytical method based on the Bernoulli sub-ODE technique. In Section 3, we illustrate the application of the analytical method and present the solutions obtained. In Section 4, we present the majority of our results in the form of two- and three-dimensional graphs. In Section 5, we investigate the numerical illustrations using two different cubic B-spline function schemes. In Section 6, we compare between analytical and numerical results. Finally, in Section 7, we provide a synopsis of our findings and draw a conclusion based on our analysis of the BZ reaction.

2 Bernoulli sub-ODE technique

The strategy of the Bernoulli sub-ODE method [19] is explained as follows: Exhibiting the main steps in the current section to illustrate the new form of the Bernoulli sub-ODE method. Presumption the model equation is given by

$$G(\zeta, \zeta_x, \zeta_t, \zeta_{xx}, \zeta_{tt}, \zeta_{xt}) = 0, \tag{2}$$

where G is a polynomial in $\zeta = \zeta(x, t)$ and its partial derivatives. Inserting the wave transformations

$$\eta = x + ct, \quad \zeta(x, t) = \zeta(\eta), \tag{3}$$

where $c > 0$ is the velocity of the wave (2) switched to the next ODE

$$Q(\zeta, \zeta', \zeta'', \zeta''', \zeta'''') = 0. \tag{4}$$

Step 1: Postulate the following finite series is the solution of (4):

$$\zeta(\eta) = \sum_{i=0}^{N} g_i (G(\eta))^i, \tag{5}$$

where $g_i \neq 0, (0 \leq i \leq N)$ are calculated from the principle of homogeneous balance to obtain the value of N and $g_N \neq 0$, then

$$G' + \lambda G = \mu G^2, \quad \lambda, \mu \neq 0, \tag{6}$$

is an ODE that has a solution $G(\eta)$ given by

$$G(\eta) = \frac{1}{\frac{\mu}{\lambda} + d e^{\lambda \eta}}. \tag{7}$$

Step 2: Inserting (5) and (6) into (4), we gain the solution of the acquired system when equating all coefficients of $G(\eta)$ to zero. The previous set will be solved using the Mathematica program.

3 Applications

Employing the wave transformation (3) on (1), we obtain the next ODE system of equations:

$$\begin{aligned} &\Theta(\eta)(-1 + r + \Theta(\eta) - r\mho(\eta)) + c\Theta'(\eta) - \Theta''(\eta) = 0, \\ &b\Theta(\eta)(-1 + \mho(\eta)) + c\mho'(\eta) - \mho''(\eta) = 0. \end{aligned} \tag{8}$$

Determine the values of M and N from (8)

(1) $\Theta(\eta)\mho(\eta)$ with $\Theta''(\eta) \Rightarrow M = 2$,

(2) $\Theta(\eta)\mho(\eta)$ with $\mho''(\eta) \Rightarrow N = 2$.

3.1 Results employing the Bernoulli sub-ODE technique

Based upon (5), the solution of (8) is stated next:

$$\begin{aligned} \Theta(\eta) &= f_0 + f_1 G(\eta) + f_2 G(\eta)^2, \\ \mho(\eta) &= m_0 + m_1 G(\eta) + m_2 G(\eta)^2. \end{aligned} \tag{9}$$

By inserting (9) into (8) and setting the coefficients with equal powers of $G(\eta)$ equal to zero, we arrive at the following system:

$$\begin{aligned} &-f_0 + rf_0 + f_0^2 - rf_0 m_0 = 0, \\ &-f_1 + rf_1 - c\lambda f_1 - \lambda^2 f_1 + 2f_0 f_1 - rf_1 m_0 - rf_0 m_1 = 0, \\ &c\mu f_1 + 3\lambda\mu f_1 + f_1^2 - f_2 + rf_2 - 2c\lambda f_2 - 4\lambda^2 f_2 + 2f_0 f_2 \\ &\qquad - rf_2 m_0 - rf_1 m_1 - rf_0 m_2 = 0, \\ &-2\mu^2 f_1 + 2c\mu f_2 + 10\lambda\mu f_2 + 2f_1 f_2 - rf_2 m_1 - rf_1 m_2 = 0, \\ &-6\mu^2 f_2 + f_2^2 - rf_2 m_2 = 0, \\ &-bf_0 + bf_0 m_0 = 0, \\ &-bf_1 + bf_1 m_0 - c\lambda m_1 - \lambda^2 m_1 + bf_0 m_1 = 0, \\ &-bf_2 + bf_2 m_0 + c\mu m_1 + 3\lambda\mu m_1 + bf_1 m_1 - 2cm_2\lambda \\ &\qquad - 4\lambda^2 m_2 + bf_0 m_2 = 0, \\ &-2m_1\mu^2 + bf_2 m_1 + 2c\mu m_2 + 10\lambda\mu m_2 + bf_1 m_2 = 0, \\ &-6\mu^2 m_2 + bf_2 m_2 = 0. \end{aligned} \tag{10}$$

Four sets of solutions are obtained when the former system of equations is solved as follows:

Set 1

$$\begin{aligned} &f_0 = 0, \quad f_1 = 0, \quad f_2 = \frac{\mu^2}{\lambda^2}, \quad m_0 = \frac{-1 + r + 6\lambda^2}{r}, \\ &m_1 = 0, \quad m_2 = \frac{\mu^2 - 6\lambda^2\mu^2}{r\lambda^2}, \\ &c = -5\lambda, \quad b = 6\lambda^2. \end{aligned} \tag{11}$$

Set 2

$$\begin{aligned} &f_0 = 1, \quad f_1 = -\frac{2\mu}{\lambda}, \quad f_2 = \frac{\mu^2}{\lambda^2}, \quad m_0 = 1, \\ &m_1 = \frac{2(-\mu + 6\lambda^2\mu)}{r\lambda}, \quad m_2 = \frac{\mu^2 - 6\lambda^2\mu^2}{r\lambda^2}, \\ &c = 5\lambda, \quad b = 6\lambda^2. \end{aligned} \tag{12}$$

Set 3

$$\begin{aligned} &f_0 = 0, \quad f_1 = -2\lambda\mu, \quad f_2 = 2\mu^2, \\ &m_0 = \frac{r^2\mu - r\mu(1 + \lambda^2) + \lambda\sqrt{r^2\mu^2(3 + \lambda^2)}}{r^2\mu}, \\ &m_1 = \frac{2}{r^2}(2r\lambda\mu - \sqrt{3r^2\mu^2 + r^2\lambda^2\mu^2}), \quad m_2 = -\frac{4\mu^2}{r}, \\ &c = -\frac{\sqrt{r^2\mu^2(3 + \lambda^2)}}{r\mu}, \quad b = 3. \end{aligned} \tag{13}$$

Set 4

$$
\begin{aligned}
&f_0 = 0, \quad f_1 = -2\lambda\mu, \quad f_2 = 2\mu^2,\\
&m_0 = \frac{r^2\mu - r\mu(1+\lambda^2) - \lambda\sqrt{r^2\mu^2(3+\lambda^2)}}{r^2\mu},\\
&m_1 = \frac{2}{r^2}\left(2r\lambda\mu + \sqrt{3r^2\mu^2 + r^2\lambda^2\mu^2}\right), \quad m_2 = -\frac{4\mu^2}{r},\\
&c = \frac{\sqrt{r^2\mu^2(3+\lambda^2)}}{r\mu}, \quad b = 3.
\end{aligned} \tag{14}
$$

The traveling wave solution is provided as follows:

$$
\begin{aligned}
\Theta(x,t) &= f_0 + f_1\left(\frac{1}{\frac{\mu}{\lambda} + de^{\lambda(x+ct)}}\right) + f_2\left(\frac{1}{\frac{\mu}{\lambda} + de^{\lambda(x+ct)}}\right)^2,\\
\mho(x,t) &= m_0 + m_1\left(\frac{1}{\frac{\mu}{\lambda} + de^{\lambda(x+ct)}}\right) + m_2\left(\frac{1}{\frac{\mu}{\lambda} + de^{\lambda(x+ct)}}\right)^2.
\end{aligned} \tag{15}
$$

4 Discussion of graphical representations

In this section, we present some graphs in two and three dimensions to show our solutions. In Figure 1, we plot graphs of (15) with set 4 (14) employing the Bernoulli sub-ODE method at $r = 1.3, d = 0.2, \mu = 0.5$ and $\lambda = 0.5$. The graphs of Θ and $\mho$ of (15) with set 2 (12) at $b = 1.56$, $b = 1.82$, and $b = 2.09$ are shown in Figure 2.

The graphs can be a very effective tool for describing and visualizing solutions to various problems, including mathematical models and systems. In the context of Figure 1, it appears that the wave being referred to is a bell-shaped soliton (dark soliton) for variable Θ and that the wave has turned down and shifted to the left (kink soliton) for variable $\mho$. This could be due to changes in the parameters of the system. Figure 2 shows the variation in variables Θ and $\mho$ as the parameter b is changed. The parameter b determines the strength of the feedback loop between the two variables Θ and $\mho$. When b is small, the feedback loop is weak and the concentration $\mho$ has little effect on the dynamics of the system. As b increases, the feedback loop becomes stronger, and the oscillations in the system become more pronounced. When b becomes very large, the system may exhibit chaotic behavior, which can be seen as irregular and unpredictable variations in the values of Θ and $\mho$.

5 Numerical method outline

We discretize the domain $[a, b]$ of the function into small intervals or knots as $\Omega : a = x_0 < x_1 < \ldots < x_{\mathcal{L}} = b$. Let the interval width be denoted by $h = \frac{b-a}{\mathcal{L}} = x_{l+1} - x_l$ for

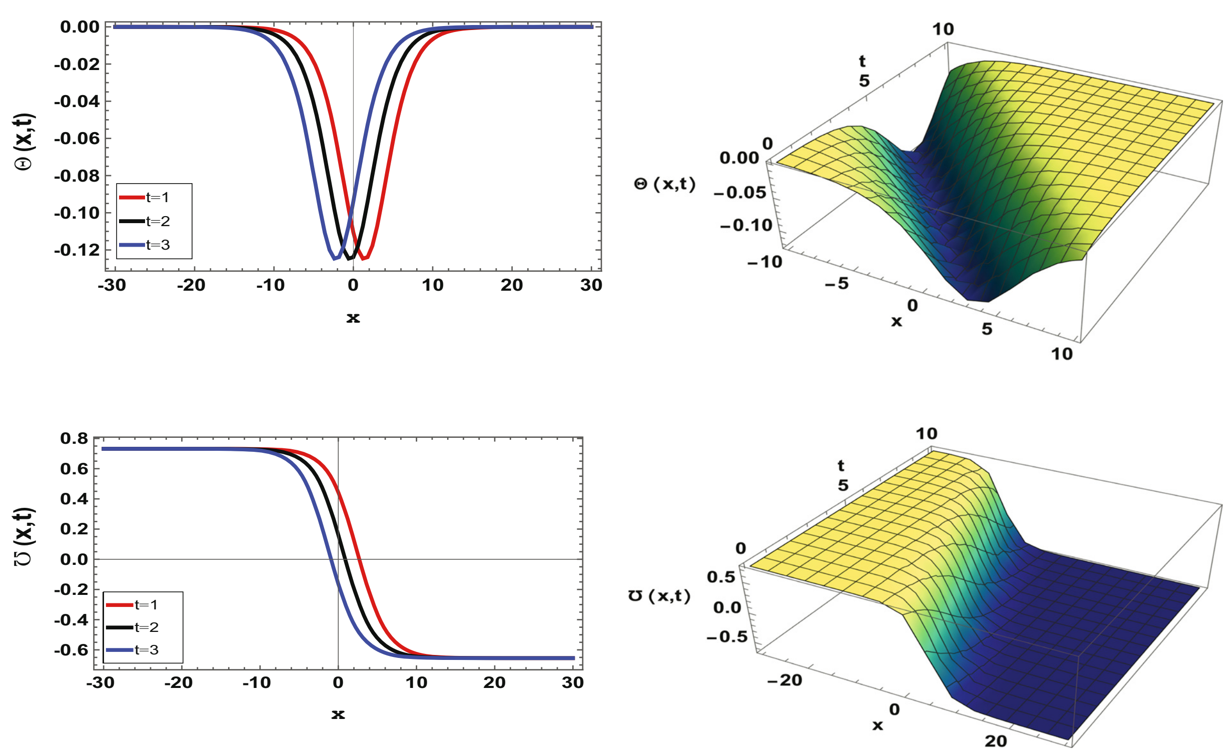

Figure 1: Graph of Θ and $\mho$ of (15) with set 4 (14) at $r = 1.3$, $d = 0.2$, $\mu = 0.5$, and $\lambda = 0.5$.

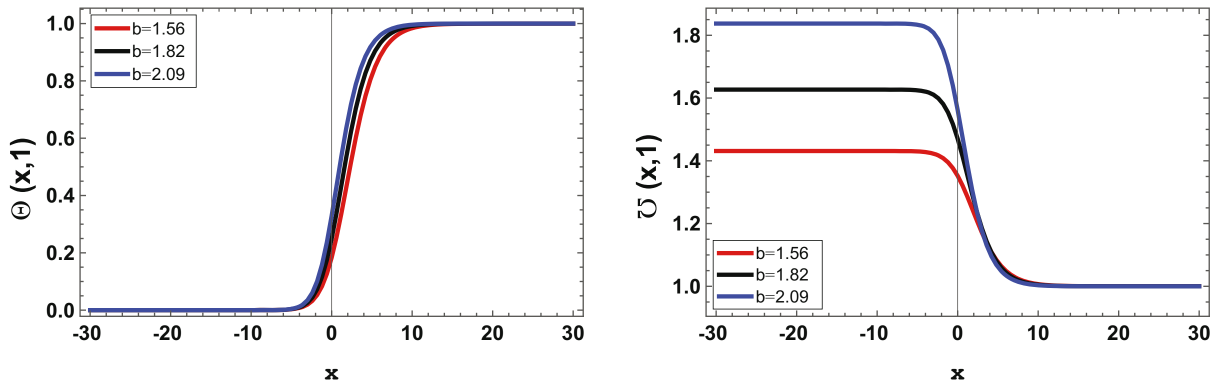

Figure 2: Graph of Θ and $\mho$ of (15) with set 2 (12) at $b = 1.56$, $b = 1.82$, and $b = 2.09$.

$l = 0, 1, \ldots, \mathcal{L}$ and let the time levels with $\Delta t > 0$ be $t_m = m\Delta t$ for $m = 0, 1, \ldots, \mathcal{M}$, where $\mathcal{M}$ is +ve integer. We use two collocation methods like exponential cubic B-spline method and trigonometric cubic B-spline method to solve the BZ equation (1) numerically.

Let the initial and boundary conditions of the BZ system (1)

$$\begin{aligned} &\Theta(x,0) = f_1(x), \quad \mho(x,0) = f_2(x), \quad a \le x \le b,\\ &\Theta(a,t) = f_3(t), \quad \Theta(b,t) = f_4(t),\\ &\mho(a,t) = f_5(t), \quad \mho(b,t) = f_6(t). \end{aligned} \tag{16}$$

Here are their outlines of two methods as follows.

5.1 Exponential cubic B-spline method

We construct the exponential cubic B-spline functions [23], $E_l(x)$, at the knots x_l, $(l = -1(1)\mathcal{L} + 1)$ can be expressed as

$$E_l(x) = \begin{cases} B_2\left((x_{l-2} - x) - \dfrac{1}{P}(\sinh(P(x_{l-2} - x)))\right) & x_{l-2} \le x \le x_{l-1},\\ A_1 + B_1(x_l - x) + C_1 \exp(P(x_l - x)) + D_1 \exp(-P(x_l - x)) & x_{l-1} \le x \le x_l,\\ A_1 + B_1(x - x_l) + C_1 \exp(P(x - x_l)) + D_1 \exp(-P(x - x_l)) & x_l \le x \le x_{l+1},\\ B_2\left((x - x_{l+2}) - \dfrac{1}{P}(\sinh(P(x_{l+2} - x)))\right) & x_{l+1} \le x \le x_{l+2},\\ 0 & \text{otherwise}, \end{cases} \tag{17}$$

where $A_1 = \frac{PhC}{PhC - S}$, $B_1 = \frac{P}{2}\left[\frac{C(C-1)+S^2}{(PhC-S)(1-C)}\right]$, $B_2 = \frac{P}{2(PhC-S)}$, $C_1 = \frac{\exp(-Ph)(1-C)+S(\exp(-Ph)-1)}{4(PhC-S)(1-C)}$, $D_1 = \frac{\exp(Ph)(C-1)+S(\exp(Ph)-1)}{4(PhC-S)(1-C)}$, $C = \cosh(Ph)$, $S = \sinh(Ph)$, and P is a free parameter.

We assume that the numerical solutions of the BZ system (1) are $\tilde{\Theta}(x,t)$ and $\tilde{\mho}(x,t)$ which are approximations to the exact solutions $\Theta(x,t)$ and $\mho(x,t)$ as follows:

$$\begin{aligned} \tilde{\Theta}(x,t) &= \sum_{l=-1}^{\mathcal{L}+1} B_l(x)\delta_l(t),\\ \tilde{\mho}(x,t) &= \sum_{l=-1}^{\mathcal{L}+1} B_l(x)\gamma_l(t), \end{aligned} \tag{18}$$

where $\delta_l(t)$ and $\gamma_l(t)$ are the time-dependent unknown quantities, $B_l(x)$ the exponential cubic B-spline function and its two derivatives $B_l'(x), B_l''(x)$ at the knots x_l are established from (17).

Using (17) and (18), we compute the numerical solutions of the BZ equation (1) and its derivatives up to second order as follows:

$$\begin{aligned} \tilde{\Theta}(x_l,t) &= (b_1)\delta_{l-1}(t) + \delta_l(t) + (b_1)\delta_{l+1}(t),\\ \tilde{\Theta}_l' &= (-b_2)(\delta_{l-1}(t) - \delta_{l+1}(t)),\\ \tilde{\Theta}_l'' &= (b_3)(\delta_{l-1}(t) - 2\delta_l(t) + \delta_{l+1}(t)), \end{aligned} \tag{19}$$

$$\begin{aligned} \tilde{\mho}(x_l,t) &= (b_1)\gamma_{l-1}(t) + \gamma_l(t) + (b_1)\gamma_{l+1}(t),\\ \tilde{\mho}_l' &= (-b_2)(\gamma_{l-1}(t) - \gamma_{l+1}(t)),\\ \tilde{\mho}_l'' &= (b_3)(\gamma_{l-1}(t) - 2\gamma_l(t) + \gamma_{l+1}(t)). \end{aligned} \tag{20}$$

where $b_1 = \frac{S - Ph}{2(PhC - S)}$, $b_2 = \frac{P(C-1)}{2(PhC-S)}$, $b_3 = \frac{P^2 S}{2(PhC-S)}$.

Substituting from (19) and (20) into (1), a general form equation is reached for the linearization technique

$$\begin{aligned}&(b_1)\dot{\delta}_{l-1}(t) + \dot{\delta}_l(t) + (b_1)\dot{\delta}_{l+1}(t) - (b_3)(\delta_{l-1}(t) - 2\delta_l(t)\\&\quad + \delta_{l+1}(t)) - ((b_1)\delta_{l-1}(t) + \delta_l(t) + (b_1)\delta_{l+1}(t))\\&\quad + r((b_1)\delta_{l-1}(t) + \delta_l(t) + (b_1)\delta_{l+1}(t)) + \mathbf{Z}_{l1}\\&\quad - r\mathbf{Z}_{l2} = 0, \qquad (21)\\&(b_1)\dot{\gamma}_{l-1l}(t) + \dot{\gamma}_l(t) + (b_1)\dot{\gamma}_{l+1}(t) - (b_3)(\gamma_{l-1}(t) - 2\gamma_l(t)\\&\quad + \gamma_{l+1}(t)) - b((b_1)\delta_{l-1}(t) + \delta_l(t) + (b_1)\delta_{l+1}(t))\\&\quad + b\mathbf{Z}_{l2} = 0,\end{aligned}$$

where $\dot{\delta}_l(t) = \frac{d\delta_l}{dt}$, $\dot{\gamma}_l(t) = \frac{d\gamma_l}{dt}$,

$$\begin{aligned}&\mathbf{Z}_{l1} = \Theta^2 = ((b_1)\delta_{l-1}(t) + \delta_l(t) + (b_1)\delta_{l+1}(t))^2,\\&\mathbf{Z}_{l2} = \Theta\mho = ((b_1)\delta_{l-1}(t) + \delta_l(t) + (b_1)\delta_{l+1}(t))((b_1)\gamma_{l-1}(t)\\&\quad + \gamma_l(t) + (b_1)\gamma_{l+1}(t)).\end{aligned}$$

We describe $\delta_l(t)$, $\gamma_l(t)$, and their derivatives with respect to time $\dot{\delta}_l(t)$, $\dot{\gamma}_l(t)$ with the finite difference method as follows:

$$\begin{aligned}&\delta_l(t) = \delta_l^m, \quad \gamma_l(t) = \gamma_l^m,\\&\dot{\delta}_l(t) = \frac{\delta_l^{m+1} - \delta_l^{m-1}}{2\Delta t}, \quad \dot{\gamma}_l(t) = \frac{\gamma_l^{m+1} - \gamma_l^{m-1}}{2\Delta t}.\end{aligned} \qquad (22)$$

Replacing $\delta_l(t)$, $\gamma_l(t)$, and their first time derivatives in (21) with (22), and eliminating four unknowns δ_{-1}, $\delta_{\mathcal{L}+1}$, γ_{-1}, $\gamma_{\mathcal{L}+1}$ via boundary conditions (16), we obtain a system $(2n + 2) \times (2n + 2)$ of nonlinear algebraic equations can be evaluated by the Mathematica program.

5.2 Trigonometric cubic B-spline method

We construct the trigonometric cubic B-spline functions [26], $T_l(x)$, at the knots x_l, $(l = -1(1)\mathcal{L} + 1)$ can be defined as

$$T_l(x) = \frac{1}{w}\begin{cases} W^3(x_{l-2}) & x_{l-2} \le x \le x_{l-1},\\ W(x_{l-2})(W(x_{l-2})Y(x_l) & x_{l-1} \le x \le x_l,\\ \quad + W(x_{l-1})Y(x_{l+1})) & \\ \quad + W^2(x_{l-1})Y(x_{l+2}) & \\ Y(x_{l+2})(Y(x_{l+2})W(x_l) & x_l \le x \le x_{l+1},\\ \quad + W(x_{l-1})Y(x_{l+1})) & \\ \quad + Y^2(x_{l+1})W(x_{l-2}) & \\ Y^3(x_{l+2}) & x_{l+1} \le x \le x_{l+2},\\ 0 & \text{otherwise}, \end{cases} \qquad (23)$$

where $w = \sin\left(\frac{h}{2}\right)\sin(h)\sin\left(\frac{3h}{2}\right)$, $W(x_l) = \sin\left(\frac{x - x_l}{2}\right)$, $Y(x_l) = \sin\left(\frac{x_l - x}{2}\right)$.

We assume that the numerical solutions of the BZ system (1) are denoted as $\tilde{\Theta}(x, t)$ and $\tilde{\mho}(x, t)$, which are approximations equivalent to the exact solutions $\Theta(x, t)$ and $\mho(x, t)$, respectively, as follows:

$$\begin{aligned}\tilde{\Theta}(x, t) &= \sum_{l=-1}^{\mathcal{L}+1} T_l(x)\alpha_l(t),\\ \tilde{\mho}(x, t) &= \sum_{l=-1}^{\mathcal{L}+1} T_l(x)\beta_l(t),\end{aligned} \qquad (24)$$

where $\alpha_l(t)$, $\beta_l(t)$ are time-dependent unknowns, and the trigonometric cubic B-spline function $T_l(x)$ and its two derivatives $T_l'(x)$, $T_l''(x)$ at the nodal points x_l are established from (23).

Using (23) and (24), we obtain the numerical solutions $\tilde{\Theta}(x, t)$ and $\tilde{\mho}(x, t)$ of the BZ equation (1) and its derivatives up to second order in terms of $\alpha_l(t)$ and $\beta_l(t)$, respectively, as follows:

$$\begin{aligned}\tilde{\Theta}(x_l, t) &= (d_1)\alpha_{l-1}(t) + (d_2)\alpha_l(t) + (d_1)\alpha_{l+1}(t),\\ \tilde{\Theta}_l' &= (-d_3)(\alpha_{l-1}(t) - \alpha_{l+1}(t)),\\ \tilde{\Theta}_l'' &= (d_4)(\alpha_{l-1}(t) + (d_5)\alpha_l(t) + (d_4)\alpha_{l+1}(t)),\end{aligned} \qquad (25)$$

$$\begin{aligned}\tilde{\mho}(x_l, t) &= (d_1)\beta_{l-1}(t) + (d_2)\beta_l(t) + (d_1)\beta_{l+1}(t),\\ \tilde{\mho}_l' &= (-d_3)(\beta_{l-1}(t) - \beta_{l+1}(t)),\\ \tilde{\mho}_l'' &= (d_4)(\beta_{l-1}(t) + (d_5)\beta_l(t) + (d_4)\beta_{l+1}(t)),\end{aligned} \qquad (26)$$

where $d_1 = \frac{\sin^2\left(\frac{h}{2}\right)}{\sin(h)\sin\left(\frac{3h}{2}\right)}$, $d_2 = \frac{2}{1 + 2\cos(h)}$, $d_3 = \frac{3}{4\sin\left(\frac{3h}{2}\right)}$,

$d_4 = \frac{3 + 9\cos(h)}{16\sin^2\left(\frac{h}{2}\right)\left(2\cos\left(\frac{h}{2}\right) + \cos\left(\frac{3h}{2}\right)\right)}$, $d_5 = \frac{3\cos^2\left(\frac{h}{2}\right)}{\sin^2\left(\frac{h}{2}\right)(2 + 4\cos(h))}$.

From (25) and (26) into (1), a general form equation is reached for the linearization technique

$$\begin{aligned}&(d_1)\dot{\alpha}_{l-1}(t) + (d_2)\dot{\alpha}_l(t) + (d_1)\dot{\alpha}_{l+1}(t) - ((d_4)\alpha_{l-1}(t)\\&\quad + (d_5)\alpha_l(t) + (d_4)\alpha_{l+1}(t)) - ((d_1)\alpha_{l-1}(t) + (d_2)\alpha_l(t)\\&\quad + (d_1)\alpha_{l+1}(t)) + r((d_1)\alpha_{l-1}(t) + (d_2)\alpha_l(t)\\&\quad + (d_1)\alpha_{l+1}(t)) + \mathbf{H}_{l1} - r\mathbf{H}_{l2} = 0, \qquad (27)\\&(d_1)\dot{\beta}_{l-1}(t) + (d_2)\dot{\beta}_l(t) + (d_1)\dot{\beta}_{l+1}(t) - ((d_4)\beta_{l-1}(t)\\&\quad + (d_5)\beta_l(t) + (d_4)\beta_{l+1}(t)) - b((d_1)\alpha_{l-1}(t)\\&\quad + (d_2)\alpha_l(t) + (d_1)\alpha_{l+1}(t)) + b\mathbf{H}_{l2} = 0,\end{aligned}$$

where $\dot{\alpha}_l(t) = \frac{d\alpha_l}{dt}$, $\dot{\beta}_l(t) = \frac{d\beta_l}{dt}$, $\mathbf{H}_{l1} = \Theta^2 = ((d_1)\alpha_{l-1}(t) + (d_2)\alpha_l(t) + (d_1)\alpha_{l+1}(t))^2$, $\mathbf{H}_{l2} = \Theta\mho = ((d_1)\alpha_{l-1}(t) + (d_2)\alpha_l(t) + (d_1)\alpha_{l+1}(t))((d_1)\beta_{l-1}(t) + (d_2)\beta_l(t) + (d_1)\beta_{l+1}(t))$.

Table 1: L_2 and L_∞ norms with time level $\Delta t = 0.1$ and step length $h = 0.2$ and values for the BZ equation using (15) and parameters of (12) and (14), respectively

t	Trigonometric cubic B-pline using set (12)				Exponential cubic B-pline using set (14)			
	$\Theta(x,t)$		$\mho(x,t)$		$\Theta(x,t)$		$\mho(x,t)$	
	L_2	L_∞	L_2	L_∞	L_2	L_∞	L_2	L_∞
0.2	6.7152×10^{-4}	3.5820×10^{-4}	2.1793×10^{-3}	5.2009×10^{-4}	4.0002×10^{-5}	2.3615×10^{-5}	1.1801×10^{-4}	6.6231×10^{-5}
0.3	8.3227×10^{-4}	3.9462×10^{-4}	2.0219×10^{-3}	5.1989×10^{-4}	3.8578×10^{-5}	2.1984×10^{-5}	1.0836×10^{-4}	5.9843×10^{-5}
0.4	1.4714×10^{-3}	8.8277×10^{-4}	4.2047×10^{-3}	1.0405×10^{-3}	8.7150×10^{-5}	6.9560×10^{-5}	3.6256×10^{-4}	4.9303×10^{-4}
0.5	9.3346×10^{-3}	1.1827×10^{-2}	5.2762×10^{-3}	4.3328×10^{-3}	1.9906×10^{-3}	3.2484×10^{-3}	1.4241×10^{-2}	2.2937×10^{-2}

We apply the finite difference method of $\alpha_l(t)$, $\beta_l(t)$, and their derivatives with respect to time $\dot{\alpha}_l(t)$, $\dot{\beta}_l(t)$ as follows:

$$\alpha_l(t) = \alpha_l^m, \quad \beta_l(t) = \beta_l^m,$$
$$\dot{\alpha}_l(t) = \frac{\alpha_l^{m+1} - \alpha_l^{m-1}}{2\Delta t}, \quad \dot{\beta}_l(t) = \frac{\beta_l^{m+1} - \beta_l^{m-1}}{2\Delta t}. \tag{28}$$

Substituting $\alpha_l(t)$, $\beta_l(t)$, and thier first time derivatives from (28) into (27) and eliminating unknowns $\alpha_{-1}, \alpha_{\mathcal{L}+1}, \beta_{-1}, \beta_{\mathcal{L}+1}$ by boundary conditions (16), we obtain a system $(2n+2) \times (2n+2)$ of nonlinear algebraic equations can be calculated by the Mathematica program.

As above, we demonstrate the efficiency and effectiveness of the numerical methods presented and compute the L_2 and L_∞ norms of the error between the numerical and exact solutions as follows:

$$L_2 = \sqrt{h\sum_{l=0}^{n}(\Theta_l^m - \tilde{\Theta}_l^m)^2} = \sqrt{h\sum_{l=0}^{n}(\mho_l^m - \tilde{\mho}_l^m)^2},$$
$$L_\infty = \max_{l=0}^{n}|\Theta_l^m - \tilde{\Theta}_l^m| = \max_{l=0}^{n}|\mho_l^m - \tilde{\mho}_l^m|. \tag{29}$$

Table 2: L_2 and L_∞ norms via an exponential B-spline method with step length $h = 1.0$, different time level Δt and values for the BZ equation using (15) and parameters of (12)

t	$\Delta t = 0.1$				$\Delta t = 0.01$			
	$\Theta(x,t)$		$\mho(x,t)$		$\Theta(x,t)$		$\mho(x,t)$	
	L_2	L_∞	L_2	L_∞	L_2	L_∞	L_2	L_∞
0.2	1.7875×10^{-3}	8.8980×10^{-4}	6.8753×10^{-4}	3.4223×10^{-4}	1.7649×10^{-3}	9.2811×10^{-4}	6.7881×10^{-4}	3.5696×10^{-4}
0.3	1.7655×10^{-3}	1.0145×10^{-3}	6.7904×10^{-4}	3.9019×10^{-4}	2.6436×10^{-3}	1.4227×10^{-3}	1.0168×10^{-3}	5.4720×10^{-4}
0.4	3.5406×10^{-3}	1.8802×10^{-3}	1.3618×10^{-3}	7.2315×10^{-4}	3.5250×10^{-3}	1.9030×10^{-3}	1.3558×10^{-3}	7.3193×10^{-4}
0.5	3.5413×10^{-3}	2.0287×10^{-3}	1.3620×10^{-3}	7.8030×10^{-4}	4.4131×10^{-3}	2.3433×10^{-3}	1.6973×10^{-3}	9.0127×10^{-4}

Table 3: L_2 and L_∞ norms via trigonometric B-spline method with step length $h = 1.0$, different time level Δt and values for the BZ equation using (15) and parameters of (14)

t	$\Delta t = 0.1$				$\Delta t = 0.01$			
	$\Theta(x,t)$		$\mho(x,t)$		$\Theta(x,t)$		$\mho(x,t)$	
	L_2	L_∞	L_2	L_∞	L_2	L_∞	L_2	L_∞
0.2	2.3897×10^{-3}	7.6357×10^{-4}	2.3713×10^{-2}	7.1354×10^{-3}	2.4482×10^{-3}	8.2541×10^{-4}	2.3721×10^{-2}	7.1029×10^{-3}
0.3	2.5338×10^{-3}	9.0546×10^{-4}	2.3726×10^{-2}	7.0598×10^{-3}	3.7364×10^{-3}	1.3069×10^{-3}	3.5521×10^{-2}	1.0625×10^{-2}
0.4	4.9227×10^{-3}	1.6647×10^{-3}	4.7213×10^{-2}	1.4195×10^{-2}	5.0800×10^{-3}	1.8356×10^{-3}	4.7279×10^{-2}	1.4129×10^{-2}
0.5	5.2898×10^{-3}	1.9896×10^{-3}	4.7356×10^{-2}	1.4039×10^{-2}	6.4874×10^{-3}	2.4116×10^{-3}	5.8994×10^{-2}	1.7614×10^{-2}

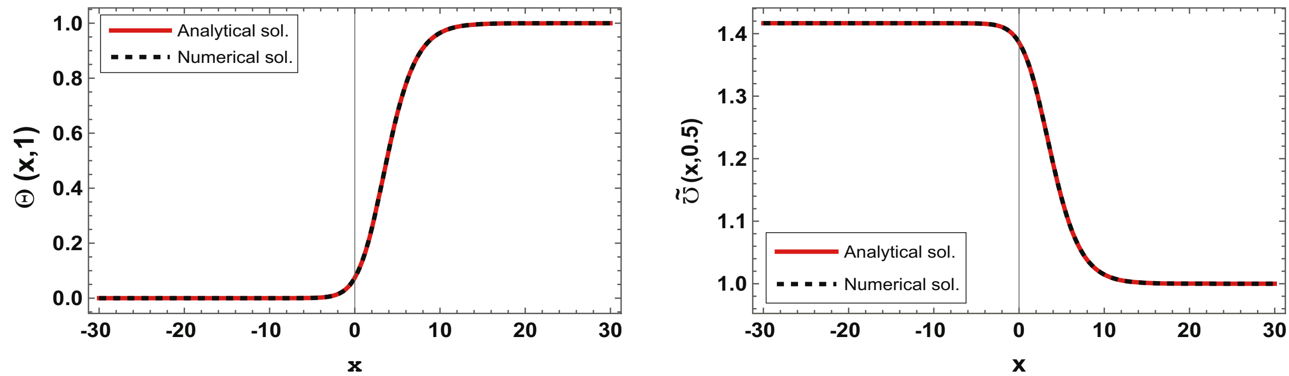

Figure 3: Numerical (exponential B-spline method) and analytical results of the BZ equation using (15) with parameters (12) at $r = 1.3$, $d = 0.2$, $\mu = 0.5$, $\lambda = 0.5$, time $t = 0.5$ with $\Delta t = 0.1$ and $h = 0.6$.

6 Comparison of analytical and numerical results

Based on the information provided, we obtain numerical results for the BZ reaction–diffusion model using the proposed numerical methods. In particular, we compute the errors L_2 and L_∞ at $r = 1.3$, $d = 0.2$, $\mu = 0.5$, $\lambda = 0.5$ for the numerical solutions of the bromous acid concentration Θ and bromide ion concentration Ʊ (15) at different step lengths and times. In Table 1, we investigate the error norms for soliton solutions of the BZ system (15) at different times with time level $\Delta t = 0.1$ and step size $h = 0.2$ via the trigonometric cubic B-spline method with parameter set (12) and the exponential cubic B-spline method with parameter set (14). The obtained results in Table 2 show the errors at different time levels by the exponential cubic B-spline method of the BZ system (15) with parameters (12), whereas the trigonometric cubic B-spline method can be applied using (15) and parameters (14) at different time levels, as shown in Table 3. Also, the graphical plots in Figures 3 and 4 show the congruence between the analytical solutions and the numerical solutions of the BZ reaction–diffusion system (15) at time $t = 0.5$ and step size $h = 0.5$ with parameters of two sets (12) and (14), respectively. Thus, we can observe the proposed numerical methods are satisfactorily accurate in solving the BZ reaction–diffusion model.

7 Conclusion

In summary, the system of equations studied in this article provides a useful model for understanding complex nonlinear systems, with a range of interesting behaviors such as oscillations and spatial patterns. The exact solutions were obtained using an analytical method such as the

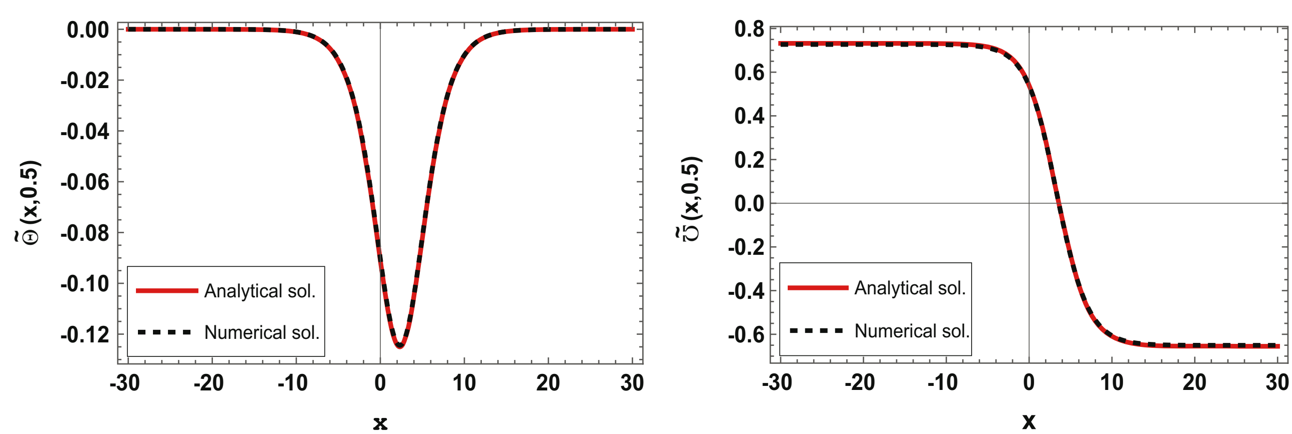

Figure 4: Numerical (trigonometric B-spline method) and analytical results of the BZ equation using (15) with parameters (14) at $r = 1.3$, $d = 0.2$, $\mu = 0.5$, $\lambda = 0.5$, time $t = 0.5$ with $\Delta t = 0.1$ and $h = 0.6$.

Bernoulli sub-ODE technique, which offers valuable insights into the system's behavior as in Figure 1 through some soliton solutions like dark and kink solitons. The effects of changing the parameters b were investigated (see Figure 2). Additionally, numerical schemes based on the exponential cubic B-spline method and trigonometric cubic B-spline method were applied to the BZ reaction–diffusion model and the results demonstrated the accuracy and efficiency of the numerical schemes as shown in Tables 1–3 and Figures 3 and 4. Future research may focus on exploring the applicability of other analytical and numerical methods to the BZ system, as well as investigating the system under different conditions and parameters. The BZ system continues to be a valuable model for studying self-organization and nonlinear dynamics in chemical systems, with potential applications in materials science, environmental monitoring, and other fields.

Acknowledgments: The authors extend their appreciation to the Deanship of Research and Graduate Studies at King Khalid University for funding this work through Large Research Project under grant number RGP2/222/45.

Funding information: This work was funded by the Deanship of Research and Graduate Studies at King Khalid University through Large Research Project under grant number RGP2/222/45.

Author contributions: All authors have accepted responsibility for the entire content of this manuscript and approved its submission.

Conflict of interest: The authors state no conflict of interest.

Data availability statement: Data sharing is not applicable to this article as no data sets were generated or analyzed during the current study.

References

[1] Murray JD. Nonlinear Differential Equations in Biology, Lectures on Models [Russian translation]. Moscow: Mir; 1983.
[2] Shanks N. Modeling biological systems: the Belousov-Zhabotinsky reaction. Found Chem. 2001;3:33–53.
[3] Hou L, Dueñas-Díez M, Srivastava R, Pérez-Mercader J. Flow chemistry controls self-assembly and cargo in Belousov-Zhabotinsky driven polymerization-induced self-assembly. Commun Chem 2019;2:139.
[4] Howell L, Osborne E, Franklin A, Hébrard EE. Pattern recognition of chemical waves: Finding the activation energy of the autocatalytic step in the Belousov-Zhabotinsky reaction. J Phys Chem B 2021;125:1667–73.
[5] Murray JD. Mathematical biology II: spatial models and biomedical applications. Third Edition. 2002.
[6] Lin G, Wan-Tong L. Travelling wavefronts of Belousov-Zhabotinskii system with diffusion and delay. Appl Math Lett. 2009;22:341–6.
[7] Murray JD. Mathematical biology. New York: Springer; 1989.
[8] Murray JD. On traveling wave solutions in a model for B-Z reaction. J Theor Biol. 1976;56:329–53.
[9] Tyson JJ. The Belousov-Zhabotinskii reaction. Lecture Notes in Biomathematics. vol. 10. New York: Springer; 1976.
[10] Ye QX, Wang MX. Travelling wave front solutions of Noyes-Field system for Belousov-Zhabotinskii reaction. Nonl Anal TMA. 1987;11:1289–302.
[11] Ye QX, Wang MX. A note on travelling wave solutions for Belousov-Zhabotinskii chemical reaction. J Beijing Inst Technol. 1989;9(4):5–9.
[12] Li ZY. The existence of travelling front solutions for reaction-diffusion system. J Partial Differ Equ. 1992;5(1):17–22.
[13] Li ZY, Ye QX. Travelling wave front solutions for reaction-diffusion systems. J Partial Differ Equ. 1991;4(3):1–14.
[14] Trofimchuk E, Pinto M, Trofimchuk S. Traveling waves for a model of the Belousov-Zhabotinsky reaction. J Differ Equ. 2013;254(9):3690–714.
[15] Basavaraja C, Huh DS, Park SH, Jeon UJ, Pierson R, Vishnuvardhan TK, et al. Bifurcation phase studies of Belousov-Zhabotinsky reaction containing oxalic acid and acetone as a mixed organic substrate in an open system. Bulletin Korean Chem Soc. 2007;28:1489–92. doi: 10.5012/bkcs.2007.28.9.1489.
[16] Manoranjan VS, Mitchell AR. A numerical study of the Belousov-Zhabotinskii chemical reaction using Galerkin finite element method. J Math Biol. 1983;16:251–60.
[17] Wang M, Xiong S, Yeeee Q. Explicit wave front solutions of Noyes-field systems for the Belousov-Zhabotinskii reaction. J Math Anal Appl. 1994;182:705–17.
[18] Quinney DA, On computing travelling wave solutions in a model for the Belousov Zhabotinskii reaction. J Inst Math Appl. 1979;23:193–201.
[19] Taghizadeh N, Akbari M, Nejhad PE. Application of Bernoulli sub-ODE method for finding travelling wave solutions of Schrodinger equation power law nonlinearity. Appl Math. 2017;12:596–603.
[20] Bilal M, Ali A, Mahmoud SR, E Tag-Eldin, Balubaid M. Fractional analysis of unsteady radiative brinkman-type nanofluid flow comprised of CoFe2O3 nanoparticles across a vertical plate. J Therm Anal Calorim. 2023;148:13869–82.
[21] Gu Y, Peng L, Huang Z, Lai Y. Soliton, breather, lump, interaction solutions and chaotic behavior for the (2+1)-dimensional KPSKR equation. Chaos Solitons Fractals. 2024;187:115351.
[22] Gu Y, Zhang X, Huang Z, Peng L, Lai Y, Aminakbari N. Soliton and lump and travelling wave solutions of the (3+1) dimensional KPB like equation with analysis of chaotic behaviors. Sci Rep. 2024;14:20966.
[23] Dag I, Ersoy O. The exponential cubic B-spline algorithm for Fisher equation. Chaos Soliton Fractal. 2016;86:101–6.
[24] Hadhoud AR, Ali KK, Shaalan MA. A septic B-spline collocation method for solving nonlinear singular boundary value problems arising in physiological models. Sci Iran E 2020;27(3):1674–84.
[25] Raslan KR, Ali KK. Numerical study of MHD-duct flow using the two-dimensional finite difference method. Appl Math Inf Sci. 2020;14:1–5.
[26] Abbas M, Majid AA, Ismail AIM, Rashid A. The application of cubic trigonometric B-spline to the numerical solution of the hyperbolic problems. Appl Math Comput. 2014;239:74–88.